Progress In Electromagnetics Research Letters, Vol. 13, 103–112, 2010

EVALUATION OF A Ni-Zn FERRITE FOR USE IN TEMPERATURE SENSORS

V. L. O. Brito

Institute for Advanced Studies, Applied Physics Division
Rodovia dos Tamoios, km 5.5, Putim, São José dos Campos,
SP 12228-001, Brazil

L. F. A. de Almeida

Faculdade de Engenharias, Arquitetura e Urbanismo
Universidade do Vale do Paraíba
Av. Shishima Hifumi, 2911, Urbanova, São José dos Campos,
SP 12244-000, Brazil

A. K. Hirata and A. C. C. Migliano

Institute for Advanced Studies, Applied Physics Division
Rodovia dos Tamoios, km 5.5, Putim, São José dos Campos,
SP 12228-001, Brazil

Abstract—This work investigates the variation of the real part of the complex magnetic permeability of a Ni-Zn ferrite for application to temperature sensors. Ferrite samples were fabricated by means of the conventional ceramic method. Zinc, nickel and iron oxides were used as raw materials. The samples were sintered at 1200, 1300, and 1400°C. The complex magnetic permeability of the samples was measured at temperatures ranging from −40°C to +50°C. The complex magnetic permeability of the samples was analyzed in the 100 kHz–100 MHz frequency range, and the temperature sensitivity of the magnetic permeability ($\partial\mu'_r/\partial T$) was analyzed at 100 kHz. The magnetic permeability variation of the ferrite permits to use it as a temperature transducer with a maximum temperature sensitivity of about $-119°C^{-1}$. The highest magnitudes of temperature sensitivity occurred between +30°C and +50°C. Therefore, the ferrite could be sensitive enough to allow temperature measurements at the human body temperature level. The results indicate that the

Corresponding author: V. L. O. de Brito (vlobrito@ieav.cta.br).

temperature range of maximum temperature sensitivity of the ferrite may be adjusted by means of appropriate selection of the fabrication parameters.

1. INTRODUCTION

Ferrites are materials of relatively low cost which are applicable to several kinds of sensors to probe, such as current [1], magnetic field [2], mechanical stresses [3], gas concentrations [4, 5], and temperature [6]. Ferrite temperature sensors for biological applications have been developed, which can monitor human body temperature [7] and also have biochemical applications [8, 9].

In temperature sensors based on the dependence of magnetic properties with temperature, the Curie temperature (T_C) of the ferrite is an important parameter to be established. Ni-Zn ferrimagnetic ferrites have T_C ranging from $-140°$C to $+570°$C approximately [10], depending on the Ni : Zn proportion. Therefore, additions of Zn and Ni change the Curie temperature in a controllable manner, thus being possible to produce ferrite material with a fine tuning of the Curie point. Cedillo et al. [11] have shown that, near T_C, the magnetic permeability (μ) of a Ni-Zn ferrite increases reaching a maximum at the Hopkinson peak. The magnetic permeability decreases steeply above the temperature that corresponds to the Hopkinson peak (T_H). In the temperature range where a steep variation rate of μ occurs the ferrites may act as a temperature transducer, such as based on the inductance variation of a circuit's component. The inductance (L) of a toroidal inductor may be calculated [12] by (1), where N is the number of coil's turns; A is the cross-section area of the ferrite core; μ_0 is the magnetic permeability of vacuum; μ_r (dimensionless) is the relative magnetic permeability of the core and r is the average radius of the ferrite core.

$$L = \frac{NA\mu_r\mu_0^2}{2\pi r} \tag{1}$$

It is well known that the magnetic permeability is a function of temperature. Therefore, the temperature variation leads to the changing of the inductance.

A usual configuration for a temperature sensor employs a resonant circuit in which the resonance frequency varies with temperature [7, 13]. This configuration allows the design of remote temperature sensors, thus eliminating the need of a power supply. The resonance frequency (ω_0) of an RLC circuit depends on the inductance, and thereby, on the $\mu_r(T)$ function, as expressed by the following

formula:

$$\omega_0 = \frac{1}{\sqrt{LC}} \tag{2}$$

In AC applications, the variation of the relative magnetic permeability with frequency is expressed by the relative complex magnetic permeability, which is composed of a real part (μ_r') and an imaginary part (μ_r''). In this case, L must be calculated using the μ_r' parameter.

The aim of this work is to analyze the variation of the real part of the complex magnetic permeability of a Ni-Zn ferrite, in temperatures between -40°C and $+50$°C, when T_C is around $+50$°C. The temperature dependence of μ_r' will be analyzed as a function of the sintering temperature.

2. EXPERIMENTAL PROCEDURE

The ferrite was formulated using raw materials in the following proportion (in wt%): 9.37% NiO, 23.83% ZnO, and 66.80% Fe_2O_3. The raw materials were wet mixed in a ball mill, dried in a furnace, uniaxially compacted in 37-mm diameter tablets, and pre-sintered at 900°C for 2 h. The compaction was used to enhance the presintering process. The tablets were manually broken and subsequently ground in a pulverizer. The powder obtained was sieved to 115 mesh. As a binder, carboxymethylcellulose (CMC) was used in a proportion of 0.6 weight% of the presintered powder mixture. The CMC was dissolved in distilled water and the powder was added to the CMC solution. The excess water was dried in a furnace and pelletization process was simulated by forcing the slightly humid powder against a nylon sieve. The pelletized powder was uniaxially compacted at 50 MPa to form cylindrical samples (external diameter (D_e) of approximately 8.3 mm, and internal diameter (D_i) of approximately 3.6 mm).

Sets of three samples were sintered for 2 h in air atmosphere at temperatures of 1200°C, 1300°C, and 1400°C. The after sintering ferrite composition was determined by means of atomic absorption spectrometry. Portions of presintered powder were sintered to undergo this analysis.

The relative complex magnetic permeability was measured in the 100 kHz–100 MHz frequency range using an impedance analyzer (Agilent 4194A). The measuring technique described in [14] was applied. The coaxial sample holder (Z-probe) used in this work allowed samples with $D_e < 7.0$ mm and $D_i > 3.05$ mm. Therefore, it was necessary to machine the samples to adjust their internal diameters to fit the sample holder. The samples' lengths were between 5.598 mm

and 8.067 mm. Before the measurements, a silver paint was applied to the internal and external cylindrical surfaces of all samples. The variation of the complex magnetic permeability with temperature was measured between −40°C and +50°C. Before measuring the magnetic permeability, the sample holder was placed inside an ESPEC SH-241 chamber for 15 minutes at each test temperature.

3. RESULTS AND DISCUSSION

Table 1 shows the results of the chemical analysis. The larger discrepancies were observed on the iron contents of the samples sintered at 1300°C and 1400°C. Zinc and oxygen losses resulting from reactions between the ferrite and the sintering atmosphere may have contributed to the increase of iron percentage. When the sintering temperature is high and the oxygen partial pressure in the sintering atmosphere is too low, zinc evaporation may occur and the Fe^{3+} ions reduce to Fe^{2+} for charge compensation. This could lead to formation of oxygen vacancies and deviations from the targeted ferrite stoichiometry [15]. This effect is usually more pronounced when sintering temperatures higher than 1200°C are used [16].

To establish the operating frequency range of the sensor's circuit it is necessary to determine the variation of the magnetic permeability with frequency. Figures 1, 2, and 3 show the real part (μ'_r) of the complex magnetic permeability measured at different temperatures. From these results, it is possible to choose an adequate reference frequency so as to obtain data to determine $\mu'_r(T)$.

At low frequencies, the test temperatures corresponding to the highest μ'_r values were: 0°C for a 1200°C sintering temperature, and +20°C for the 1300°C and 1400°C sintering temperatures.

Table 1. Results of chemical analysis (wt%) of the ferrite powders sintered at different temperatures.

Element	Sintered at 1200°C	Sintered at 1300°C	Sintered at 1400°C
Fe	45.23 (± 0.94)	51.29 (±0.81)	49.14 (±0.98)
Ni	6.05 (±1.29)	5.36 (±0.27)	6.74 (±1.28)
Zn	20.25 (±1.00)	18.86 (±0.26)	19.15 (±1.01)
O	28.47*	24.49*	24.97*

*Estimated as the remainder for 100% completion.

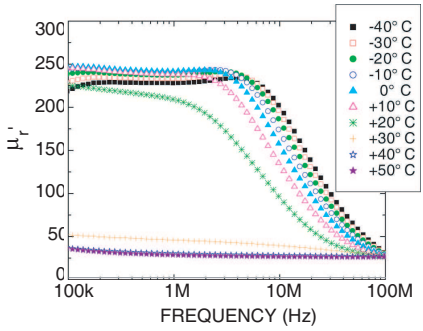

Figure 1. Variation of μ_r' with frequency at each test temperature. Sintering temperature: 1200°C.

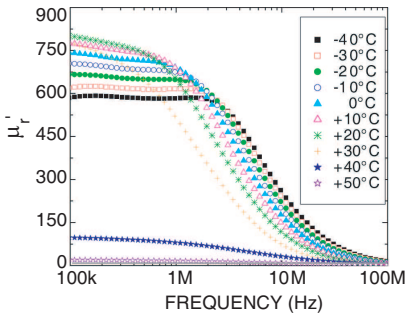

Figure 2. Variation of μ_r' with frequency at each test temperature. Sintering temperature: 1300°C.

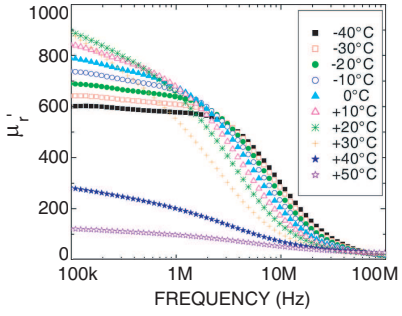

Figure 3. Variation of μ_r' with frequency at each test temperature. Sintering temperature: 1400°C.

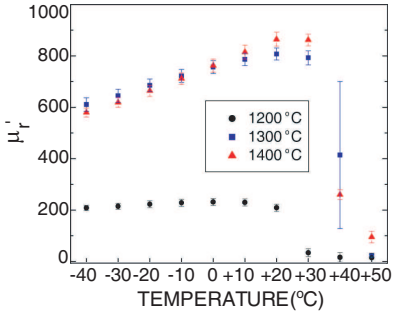

Figure 4. Variation of μ_r' (at 100 kHz) with temperature for each sintering temperature.

The frequency range of higher μ_r' frequency stability varied with sintering temperature and was within 100 kHz–4 MHz. The lower test temperatures yielded more stable μ_r' values. The temperature interval of highest μ_r' temperature sensitivity, in that frequency range, varied with sintering temperature and was within +10 to +50°C. The frequency chosen for evaluation of the ferrite as temperature sensor was 100 kHz because of high temperature sensitivity at this frequency and low variation of μ_r' with frequency near this value. This behavior of μ_r' makes the sensor less sensitive to electromagnetic interferences.

Comparing Figures 1, 2, and 3, one can observe that μ_r' variation with temperature at 100 kHz is more pronounced for the samples sintered at 1300°C and 1400°C. Near 100 kHz, the μ_r' variation with

frequency of the sample sintered at 1300°C is smaller than the one observed for the sample sintered at 1400°C. Therefore, the 1300°C sintering temperature provides the most interesting combination of temperature sensitivity/frequency stability of μ'_r in frequencies near 100 kHz.

Figure 4 shows the average μ'_r values at 100 kHz (and the corresponding standard deviations) obtained for each set of three ferrite samples. The temperatures corresponding to the Hopkinson peak were between +10°C and +30°C for the samples sintered at 1300 and 1400°C, and between −10°C and +10°C for the samples sintered at 1200°C. For $T < T_H$ the relationship between μ'_r and T was approximately linear and $\partial\mu'_r/\partial T$ (temperature sensitivity of μ'_r) increased with sintering temperature. The observed configuration of the curves is typical of ferrimagnetic materials [17].

The 1400°C sintering temperature yielded the highest temperature sensitivity and a linear relationship between μ'_r and T, in a wide temperature range below T_H. The linear fit of the data obtained at $T < T_H$ for a sample sintered at 1400°C resulted in $\mu'_r = 760.73 + 4.93T$ with a correlation coefficient $R = 1.00$ and a temperature sensitivity of approximately $+5°C^{-1}$. It is important to notice that the ferrite may present the same magnetic permeability value at two distinct temperatures when the actual temperature crosses T_H. This behavior can be observed on Figure 4: the same μ'_r value is found, for example, at +10°C and +30°C for the samples sintered at 1300°C. Thus, it may become a problem if the actual temperature being measured unexpectedly exceeds the operation limits of the sensor.

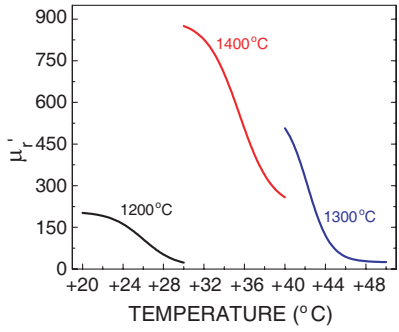

Figure 5. Sigmoidal fits of the μ'_r data in the temperature ranges of estimated maximum temperature sensitivity.

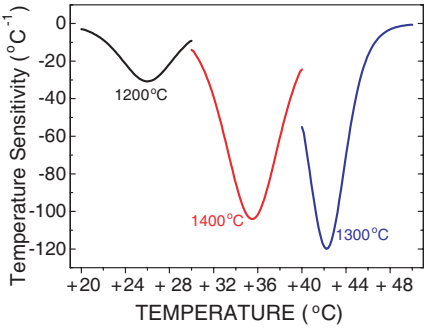

Figure 6. Derivatives (temperature sensitivity of μ'_r) of the curves on Figure 5.

Figure 4 shows that a steep drop of μ'_r occurs for $T > T_H$. It can also be seen that, in some shorter temperature ranges above T_H, the temperature sensitivity reached the highest levels. Taking the average μ'_r values as reference, such temperature ranges were +20 to +30°C for a sintering temperature of 1200°C, +30 to +40°C for sintering at 1400°C, and +40 to +50°C for sintering at 1300°C. New μ'_r measurements were made in these temperature ranges, in steps of 2°C. The sigmoidal fits of the data obtained from one sample per sintering temperature are shown on Figure 5. The correlation coefficients of the fits were 1.000. The $\mu'_r \times T$ relationship was approximately linear only in some narrow temperature ranges, with amplitudes shorter than 4°C.

The $\partial\mu'_r/\partial T$ parameters were calculated taking the derivative of the sigmoidal functions on Figure 5. Figure 6 shows the derivatives obtained. The maximum $\partial\mu'_r/\partial T$ values for these samples were $-119°C^{-1}$ for a sintering temperature of 1300°C, followed by $-104°C^{-1}$ for a sintering temperature of 1400°C, and $-30°C^{-1}$ for a sintering temperature of 1200°C. The high temperature sensitivity near +40°C, presented by the sample sintered at 1300°C, may justify the highly scattered results at +40°C previously observed on Figure 4.

The more homogeneous the chemical composition of the material [11], the steeper the slope of the μ'_r drop at $T > T_H$. Therefore, the sintering conditions of a Ni-Zn ferrite can influence its temperature sensitivity which tends to decrease in the following situations:

- Low sintering temperature and/or short sintering times: such conditions do not favor diffusion and the completion of the reactions, thereby, affecting the composition homogeneity of the sample;
- High sintering temperature and long sintering times: these conditions favors zinc volatilization, leading to composition gradients in the ferrite.

Figure 4 shows that, for $T > T_H$, as the ferrite temperature sensitivity is enhanced, the transducer's ranges of application are shortened. Also, as the temperature sensitivity is no longer constant, further output signal processing is required to measure the temperature. In homogeneous materials, the nearly vertical drop of μ'_r at $T > T_H$ restricts their temperature range of application. Thus, the temperature range of maximum sensitivity could be enlarged by a judicious control of the material's heterogeneity.

The design of the temperature sensor must consider the impairment of the transducer's dynamic sensitivity because of the ferrite low thermal conductivity (about $4\,W°C^{-1}m^{-1}$ [18]). Low-mass transducers, such as films, could minimize this problem.

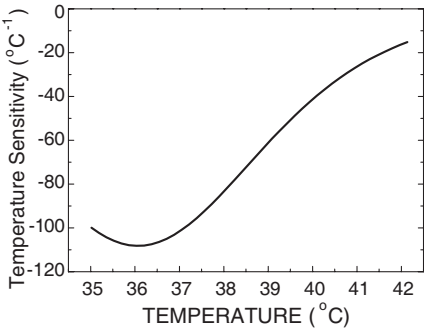

Figure 7. μ_r' temperature sensitivity of a sample sintered at 1300°C. The curve is the derivative of a μ_r' sigmoidal fit.

Adjusting the sintering conditions would make this ferrite a highly sensitive transducer for measurements in the human body temperature range. Figure 7 shows the temperature sensitivity curve of a sample sintered at 1300°C, obtained from μ_r' measurements between +35°C and +42°C in steps of 2°C. This particular sample showed temperature sensitivity varying from $-15°C^{-1}$ at +42°C to $-108°C^{-1}$ at +36°C. Note that the results don't match precisely the curve on Figure 6 because the high sensitivity led to high scattering in measurements taken from different samples.

4. CONCLUSION

At temperatures below the Hopkinson peak, which occurred between −10°C and +30°C, μ_r' of the Ni-Zn ferrite increased linearly with temperature, with a maximum temperature sensitivity of $+5°C^{-1}$. The maximum temperature sensitivity occurred above T_C and reached $-119°C^{-1}$ in a temperature range comprehending human body temperatures. The results of this work indicate that the temperature sensitivity of the ferrite may be tuned by optimizing the sintering conditions.

ACKNOWLEDGMENT

The authors would like to acknowledge:

- Materials Division of the Institute for Aeronautics and Space (AMR-IAE) — Brazil for carrying out the chemical analysis;
- CNPq for the financial support;

- Dr. Carlos Rodolfo Silveira Stopa for the suggestions given during the preparation of this work.

REFERENCES

1. Brito, V. L. O., A. C. C. Migliano, L. V. Lemos, and F. C. L. Melo, "Ceramic processing route and characterization of a Ni-Zn ferrite for application in a pulsed-current monitor," *Progress In Electromagnetics Research*, PIER 91, 303–318, 2009.
2. Sedlar, M., V. Matejec, and I. Paulicka "Optical fibre magnetic field sensors using ceramic magnetostrictive jackets," *Sens. Act. A*, Vol. 84, 297–302, 2000.
3. Bieńkowski, A. and R. Szewczyc, "The possibility of utilizing the high permeability magnetic materials in construction of magnetoelastic stress and force sensors," *Sens. Act. A*, Vol. 113, 270–276, 2004.
4. Zhang, G., C. Li, F. Cheng, and J. Chen, "$ZnFe_2O_4$ tubes: Synthesis and application to gas sensors with high sensitivity and low-energy consumption," *Sens. Act. B*, Vol. 120, 403–410, 2007.
5. Arshak, K. and I. Gaidan, "Development of a novel gas sensor based on oxide thick films," *Mat. Sci. Eng. B*, Vol. 118, No. 1–3, 44–49, 2005.
6. Shin, H.-S., "Ferrite device for sensing temperature," U.S. Patent No. 5,775,810, 1998.
7. Kim, Y. H., S. Hashi, K. Ishiyama, K. I. Arai, and M. Inoue, "Remote temperature sensing system using reverberated magnetic flux," *IEEE Trans. Magn.*, Vol. 36, No. 5, 3643–3645, 2000.
8. Osada, H., K. Seki, H. Matsuki, S. Kikuchi, and K. Murakami, "Temperature-sensitive magnetic thin-film for micro sensor," *IEEE Trans. Magn.*, Vol. 31, No. 6, 3164–3166, 1995.
9. Osada, H., S. Chiba, H. Oka, H. Hatafuku, N. Tayama, and K. Seki, "Non-contact magnetic temperature sensor for biochemical applications," *J. Magn. Magn. Mater.*, Vol. 272–276, e1761–e1762, 2004.
10. Valenzuela, R., *Magnetic Ceramics*, 131, Cambridge University Press, Cambridge, 1994.
11. Cedillo, E., J. Ocampo, V. Rivera, and R. Valenzuela, "An apparatus for the measurement of initial magnetic permeability as a function of temperature," *J. Phys. E: Sci. Inst.*, Vol. 13, No. 4, 383–386, 1980.
12. Brito, V. L. O., "Seleção, elaboração e caracterização de ferritas

Ni-Zn para aplicação em monitores de corrente pulsada," Ph.D. Thesis, 38, São José dos Campos, Instituto Tecnológico de Aeronáutica, 2007.

13. Naoe, M., R. Takahashi, T. Omura, Y. Hotta, T. Sato, K. Yamasawa, and Y. Miura, "Basic investigation of microtemperature sensor by means of a novel transmission-line technique using a temperature-sensitive Li-Zn-Cu ferrite substrate," *J. Magn. Magn. Mater.*, Vol. 320, e949–e953, 2008.
14. Côrtes, A. L., A. C. C. Migliano, V. L. O Brito, and A. J. F. Orlando, "Practical aspects of the characterization of ferrite absorber using one-port device at RF frequencies," *PIERS Proceedings*, 683–687, Beijing, China, March 26–30, 2007.
15. Verma, A. and R. Chatterjee, "Effect of zinc concentration on the structural, electrical and magnetic properties of mixed Mn-Zn and Ni-Zn ferrites synthesized by the citrate precursor technique," *J. Magn. Magn. Mater.*, Vol. 306, 313–320, 2006.
16. Gul, I. H., W. Ahmed, and A. Maqsood, "Electrical and magnetic characterization of nanocrystalline Ni-Zn ferrite synthesis by co-precipitation route," *J. Magn. Magn. Mater.*, Vol. 320, 270–275, 2008.
17. Gignoux, D. and M. Schlenker, *Magnetism: Fundamentals*, 129, Springer, New York, 2005.
18. Goldman, A., *Modern Ferrite Technology*, 398, Springer, New York, 2006.